15th World Congress on Computational Mechanics (WCCM-XV)
8th Asian Pacific Congress on Computational Mechanics (APCOM-VIII)
Virtual Congress: 31 July – 5 August 2022
S. Koshizuka (Ed.)

UNCONDITIONALLY STABLE DYNAMIC ANALYSIS OF MULTI-PATCH KIRCHHOFF-LOVE SHELLS IN LARGE DEFORMATIONS

DOMENICO MAGISANO[1], LEONARDO LEONETTI[1] AND GIOVANNI GARCEA[1]

[1] University of Calabria
87036, Rende (Cosenza), Italy
domenico.magisano@unical.it

Key words: Nonlinear dynamics, Large deformation, Stability, Kirchhoff-Love

Abstract. *This work presents a numerical framework for long dynamic simulations of structures made of multiple thin shells undergoing large deformations. The C1-continuity requirement of the Kirchhoff-Love theory is met in the interior of patches by cubic NURBS approximation functions with membrane locking avoided by patch-wise reduced integration. A simple penalty approach for coupling adjacent patches, applicable also to non-smooth interfaces and non-matching discretization is adopted to impose translational and rotational continuity. A time-stepping scheme is proposed to achieve energy conservation and unconditional stability for general nonlinear strain measures and penalty coupling terms, like the nonlinear rotational one for thin shells. The method is a modified mid-point rule with the internal forces evaluated using the average value of the stress at the step end-points and an integral mean of the strain-displacement tangent operator over the step computed by time integration points.*

1 INTRODUCTION

One-step implicit time integration methods such as Newmark's schemes are only conditionally stable when used in large deformation analyses [1]. Simo and Tarnow proposed a simple method that guarantees unconditional stability by conserving the algorithmic energy in elastodynamics [2]. However, energy conservation is lost for other structural models as the Kirchhoff-Love theory, more efficient in the terms of spatial DOFs for thin shell problems, where the strain-displacement relationship is no longer quadratic. This work presents a numerical framework for long term dynamic simulations of structures made of multiple thin shells undergoing large deformations. The C1-continuity requirement of the Kirchhoff-Love theory is met in the interior of patches by cubic NURBS approximation functions, according to the isogeometric concept, with membrane locking avoided by patch-wise reduced integration [4]. A simple penalty approach for coupling adjacent patches, applicable to either smooth or non-smooth interfaces and either matching or non-matching discretizations is adopted to impose translational and rotational continuity [5]. The time-stepping scheme of Simo and Tarnow is generalized to achieve energy conservation for generally nonlinear strain measures and penalty coupling terms, like the nonlinear rotational one for thin shells. The method is based on a particular integral mean of the internal forces over the step, that includes Simo and Tarnow's method as a reduced quadrature rule, and has unconditional stability.

2 STABLE TIME INTEGRATION IN LARGE DEFORMATION DYNAMICS

2.1 Large deformation dynamic problem with general nonlinear strain measure

Let us consider a generic elastic body characterized by a linear elastic constitutive law

$$\boldsymbol{\sigma} = \mathbf{C}\boldsymbol{\varepsilon}$$

where $\boldsymbol{\sigma}$ is the vector collecting the stress/generalized stress components, $\boldsymbol{\varepsilon}$ is the vector collecting the strain/generalized strain components and $\mathbf{C}$ is the constitutive matrix. The strain is linked to the displacement field $\boldsymbol{u}$ by means of a differential operator generally nonlinear in $\boldsymbol{u}$:

$$\boldsymbol{\varepsilon} = \boldsymbol{\varepsilon}(\boldsymbol{u}) \tag{1}$$

Applying a spatial discretization technique, for instance the finite element method or the isogeometric analysis, the displacement is approximated at element level as

$$\boldsymbol{u} = \mathbf{N}_u \mathbf{u}_e$$

where matrix $\mathbf{N}_u$ collect the spatial shape functions. The strain energy of the body can be expressed as a sum of element contributions as $\Phi \equiv \sum_e \Phi_e(\mathbf{u}_e)$, with

$$\Phi_e(\mathbf{u}_e) \equiv \int_{\Omega_e} \left(\frac{1}{2} \boldsymbol{\varepsilon}^T \mathbf{C} \boldsymbol{\varepsilon} \right) d\Omega_e \tag{2}$$

where Ω_e is the element domain. The first variation of the strains in Eq.(1) can be written as

$$\delta\boldsymbol{\varepsilon} = \mathbf{B}(\mathbf{u}_e)\delta\mathbf{u}_e \tag{3}$$

where matrix $\mathbf{B}$ is the strain-displacement tangent operator. The first variation of the element strain energy

$$\begin{aligned} \Phi_e(\mathbf{u}_e)'\delta\mathbf{u}_e &\equiv \int_{\Omega_e} \left(\delta\boldsymbol{\varepsilon}^T \mathbf{C} \boldsymbol{\varepsilon} \right) d\Omega_e \\ &= \delta\mathbf{u}_e^T \int_{\Omega_e} \left(\mathbf{B}(\mathbf{u}_e)^T \mathbf{C} \boldsymbol{\varepsilon}(\mathbf{u}_e) \right) d\Omega_e = \delta\mathbf{u}_e^T \mathbf{s}_e(\mathbf{u}_e) \end{aligned} \tag{4}$$

allows us to define the element internal force vector

$$\mathbf{s}_e(\mathbf{u}_e) \equiv \int_{\Omega_e} \left(\mathbf{B}(\mathbf{u}_e)^T \boldsymbol{\sigma}(\mathbf{u}_e) \right) d\Omega_e \quad \text{with} \quad \boldsymbol{\sigma}(\mathbf{u}_e) = \mathbf{C}\boldsymbol{\varepsilon}(\mathbf{u}_e) \tag{5}$$

Similarly, the velocity field $\boldsymbol{v}$ is approximated consistently as

$$\boldsymbol{v} = \mathbf{N}_u \mathbf{v}_e$$

where $\mathbf{v}_e$ are the discrete velocity DOFs. The kinetic energy is then sum of element contributions $T(\mathbf{v}) \equiv \sum_e T_e(\mathbf{v}_e)$ with

$$T_e(\mathbf{v}_e) \equiv \int_{\Omega_e} \left(\frac{1}{2} \boldsymbol{v}^T \boldsymbol{\Xi} \boldsymbol{v} \right) d\Omega_e = \frac{1}{2} \mathbf{v}_e^T \mathbf{M}_e \mathbf{v}_e \tag{6}$$

where $\boldsymbol{\Xi}$ is a diagonal matrix with the mass density associated to each component of $\boldsymbol{\nu}$, which can be different for examples when $\boldsymbol{\nu}$ collects both translational and rotational velocities, and $\mathbf{M}_e$ is the element mass matrix.

After a standard assemblage process, the semi-discrete equations of motion for the discretized body can be written, neglecting the damping, in terms of the global DOFs $\mathbf{u}$ and $\mathbf{v}$ as

$$\begin{cases} \mathbf{v} = \dot{\mathbf{u}} \\ \mathbf{M}\dot{\mathbf{v}} + \mathbf{s}(\mathbf{u}) = \mathbf{f} \end{cases} \tag{7}$$

where a dot denotes time derivative and $\mathbf{f}$ is the discrete load vector, while the total energy of the system is

$$\Pi(\mathbf{u},\mathbf{v}) \equiv T(\mathbf{v}) + \Phi(\mathbf{u}) - \mathbf{u}^T\mathbf{f}. \tag{8}$$

2.2 One-step time integration

Letting $\alpha = \dfrac{t-t_0}{t_1-t_0}$, a one-step time integration scheme can be obtained introducing the approximation in time for $\mathbf{u}$ and $\mathbf{v}$ over the time step $[t_0,t_1]$ with $t_1 = t_0 + \Delta t$:

$$\begin{cases} \mathbf{v}(\alpha) = \mathbf{v}_0 + \alpha(\mathbf{v}_1 - \mathbf{v}_0) \\ \mathbf{u}(\alpha) = \mathbf{u}_0 + \alpha(\mathbf{u}_1 - \mathbf{u}_0) \end{cases} \tag{9}$$

The semi-discrete equations of motion (7) can be then rewritten in discrete form as

$$\begin{cases} \bar{\mathbf{v}} = \dfrac{\mathbf{u}_1 - \mathbf{u}_0}{\Delta t} \\ \mathbf{M}\dfrac{\mathbf{v}_1 - \mathbf{v}_0}{\Delta t} + \bar{\mathbf{s}}(\mathbf{u}) = \bar{\mathbf{p}} \end{cases} \tag{10}$$

where $\bar{\mathbf{v}}$, $\bar{\mathbf{s}}$ and $\bar{\mathbf{p}}$ are representative value of $\mathbf{v}(\alpha)$, $\mathbf{s}(\alpha)$ and $\mathbf{p}(\alpha)$ over the step. For $\bar{\mathbf{v}}$ and $\bar{\mathbf{p}}$, a simple and natural choice is to define them as the integral mean of the corresponding function, so that we have

$$\begin{cases} \dfrac{\mathbf{v}_1 + \mathbf{v}_0}{2} = \dfrac{\mathbf{u}_1 - \mathbf{u}_0}{\Delta t} \\ \mathbf{M}\dfrac{\mathbf{v}_1 - \mathbf{v}_0}{\Delta t} + \bar{\mathbf{s}}(\mathbf{u}) = \bar{\mathbf{p}} \quad \text{with} \quad \bar{\mathbf{p}} \equiv \displaystyle\int_0^1 \mathbf{p}(\alpha)d\alpha \end{cases} \tag{11}$$

We can get $\mathbf{v}_1$ from the first of Eq. (11) and substitute it into the second, so obtaining the final form of the discrete equations of motion in terms of the only unknowns $\mathbf{u}_1$:

$$2\mathbf{M}\frac{\mathbf{u}_1 - \mathbf{u}_0 - \mathbf{v}_0\Delta t}{\Delta t^2} + \bar{\mathbf{s}}(\mathbf{u}) = \bar{\mathbf{p}} \tag{12}$$

Different choices are possible for $\bar{\mathbf{s}}(\mathbf{u})$.

2.3 The new integration scheme

Now, we present a new one-step integration method aimed at preserving energy as well as the strain-displacement compatibility at the step end-point for generally nonlinear strain measures. Starting for the

time interpolation in Eq. (9), the idea is to generalize the Simo and Tarnow method as follows. Firstly, at each spatial integration point, a representative value of the strain-displacement tangent operator is computed as integral mean of $\mathbf{B}(\mathbf{u})$ over the step:

$$\bar{\mathbf{B}} = \int_0^1 \mathbf{B}(\mathbf{u}(\alpha))d\alpha \approx \sum_{n=1}^{N_t} \mathbf{B}(\mathbf{u}(\alpha_n))\varpi_n \tag{13}$$

Then, the representative internal force vector of the step is evaluated as

$$\bar{\mathbf{s}}(\mathbf{u}) \equiv \int_V \bar{\mathbf{B}}^T \bar{\boldsymbol{\sigma}} dV \quad \text{with} \quad \bar{\boldsymbol{\sigma}} = \mathbf{C}\frac{\boldsymbol{\varepsilon}(\mathbf{u}_1)+\boldsymbol{\varepsilon}(\mathbf{u}_0)}{2}. \tag{14}$$

with α_n and ϖ_n temporal position and weight of the nth time integration point respectively. So, the scheme is very similar to Simo and Tarnow's one [2]. The difference is the integral mean $\bar{\mathbf{B}}$ instead of the mean value $\mathbf{B}_{\frac{1}{2}}$. This choice is the crucial idea to achieve energy conservation for arbitrarily nonlinear strain-displacement laws. Indeed, it is easy to verify that

$$\boldsymbol{\varepsilon}_1 - \boldsymbol{\varepsilon}_0 = \Delta t \int_0^1 \dot{\boldsymbol{\varepsilon}} d\alpha = \Delta t \int_0^1 \mathbf{B}(\mathbf{u}(\alpha))\dot{\mathbf{u}} d\alpha = \bar{\mathbf{B}}(\mathbf{u}_1 - \mathbf{u}_0) \tag{15}$$

and then energy conservation holds independently of the strain measure nonlinearity:

$$(\mathbf{u}_1 - \mathbf{u}_0)^T \bar{\mathbf{s}}(\mathbf{u}) \equiv \int_V (\mathbf{u}_1 - \mathbf{u}_0)^T \bar{\mathbf{B}}^T \mathbf{C}\frac{\boldsymbol{\varepsilon}(\mathbf{u}_1)+\boldsymbol{\varepsilon}(\mathbf{u}_0)}{2} dV = \frac{1}{2}\int_V \left\{\boldsymbol{\varepsilon}_1^T \mathbf{C}\boldsymbol{\varepsilon}_1 - \boldsymbol{\varepsilon}_0^T \mathbf{C}\boldsymbol{\varepsilon}_0\right\} dV = \Phi(\mathbf{u}_1) - \Phi(\mathbf{u}_0) \tag{16}$$

Clearly, the energy conservation tends to be exact by increasing the number of time integration points in (13). For example the Simo and Tarnow method, that is only approximately conserving for nonlinear measures other than quadratic, can be seen as a reduced integration of the proposed method where the integral mean of $\mathbf{B}$ is approximated by a single Gauss point in time. Although the number of time integration point for a converged $\bar{\mathbf{B}}$ is a-priori unknown for general problems, a few time points, as shown in the numerical examples, gives energy conservation for practical applications and time steps. Compared to the full integration of $\mathbf{s}(\mathbf{u})$ discussed in [1], the number of time integration points required is usually lower, because only $\mathbf{B}(\mathbf{u})$ in now integrated instead of the more nonlinear term $\mathbf{B}(\mathbf{u})^T\boldsymbol{\sigma}(\mathbf{u})$. More importantly, in our proposal the internal forces are evaluated using only the stress at the end-points of the step, avoiding the inaccuracies caused by the inner stress derived from the displacement. With respect to the Sansour et al. method [3], the proposal fulfill exactly the strain-displacement relation at the step end-points and results to be unconditionally stable.

2.4 Extension to nonlinear multi-body coupling laws

Multi-body coupling laws can be generically written as

$$\boldsymbol{\varepsilon}_c(\boldsymbol{u}) = \mathbf{0} \quad \forall \mathbf{x} \in \ell \tag{17}$$

where ℓ denotes the boundary of the bodies where the coupling occurs. Without introducing additional DOFs for the Lagrange multipliers and upsetting the structure of existing finite element packages, general couplings expressed by Eq. (17) can be easily imposed in penalty form by adding to the strain energy of the system the penalty term

$$\Phi_c(\mathbf{u}) \equiv \int_\ell \frac{1}{2}\boldsymbol{\varepsilon}_c(\mathbf{u})^T \mathbf{C}_c \boldsymbol{\varepsilon}_c(\mathbf{u}) ds \tag{18}$$

where $\boldsymbol{\varepsilon}_c(\mathbf{u})$ is interpreted as a pseudo-strain that is constrained to negligible values by a stiff pseudo-constitutive matrix $\mathbf{C}_c = a\hat{\mathbf{C}}_c$ with matrix $\hat{\mathbf{C}}_c$ chosen on the basis of the actual materials and geometry of the coupled bodies [6], so that the penalty factor a defines how small we want the penalty energy to be with respect to strain energy of the system. For general structural problems and coupling laws, the constraint tends to be satisfied point-wise with the mesh refinement as in the Lagrange multipliers approach for a sufficiently high penalty factor. The penalty coupling is useful to model real complex structures with generic interfaces and non-matching discretizations [5]. The gradient of $\Phi_c(\mathbf{u})$ provides the equivalent internal forces due to the coupling

$$\mathbf{s}_c(\mathbf{u}) \equiv \int_\ell \mathbf{B}_c(\mathbf{u})^T \boldsymbol{\sigma}_c ds \quad \text{with} \quad \boldsymbol{\sigma}_c \equiv \mathbf{C}_c \boldsymbol{\varepsilon}_c(\mathbf{u}) \tag{19}$$

that has the same form of the element internal force vector with $\mathbf{B}_c(\mathbf{u})$ the tangent pseudo-strain/displacement operator. This is then assembled together with the element ones to obtain the global internal force vector to be used in global equations of motion Eq. (7). In this framework, the time integration method developed in the previous subsection can be directly applied to problems with generally nonlinear multi-body couplings, guarantying energy conservation and unconditional stability.

3 ISOGEOMETRIC KIRCHHOFF–LOVE SHELL MODEL

A Total Lagrangian formulation identifies material points on the middle surface of the current configuration in terms of their position vector $\mathbf{X}(\xi,\eta)$ in the reference configuration and the displacement field $\boldsymbol{u}(\xi,\eta)$:

$$\mathbf{x}(\xi,\eta) = \mathbf{X}(\xi,\eta) + \boldsymbol{u}(\xi,\eta) \tag{20}$$

where $\zeta = [\xi,\eta]$ denotes convective curvilinear shell coordinates with (ξ,η) representing in-plane coordinates. The middle surface covariant basis vectors in the undeformed and deformed configuration are obtained from the corresponding partial derivatives of the position vectors $\mathbf{X}$ and $\mathbf{x}$, respectively

$$\mathbf{G}_i = \mathbf{X}_{,i}\,, \qquad g_i = \mathbf{x}_{,i} = \mathbf{G}_i + \boldsymbol{u}_{,i} \qquad \text{with } i = 1,2\,, \tag{21}$$

where $()_{,i}$ denotes the partial derivative with respect to the i-th component of ζ, while the unit normals are

$$\mathbf{A}_3 = \frac{\mathbf{G}_3}{\|\mathbf{G}_3\|}, \quad \mathbf{a}_3 = \frac{g_3}{\|g_3\|} \quad \text{with} \quad \mathbf{G}_3 = \mathbf{G}_1 \times \mathbf{G}_2, \quad g_3 = g_1 \times g_2, \tag{22}$$

which corresponds to the Kirchhoff-Love (KL) shell assumption that the director remains straight and normal to the mid-surface during deformation.

The contravariant basis vectors follow from the dual basis condition: $g_i \cdot g^j = \mathbf{G}_i \cdot \mathbf{G}^j = \delta_i^j$ with $i,j = 1,2$. Exploiting Eq.(22), the transverse shear strains vanish and the Green-Lagrange strain tensor reduces to

$$\mathbf{E} = \bar{E}_{ij}\mathbf{G}^i \otimes \mathbf{G}^j \quad i,j = 1,2 \tag{23}$$

where $\bar{E}_{ij}$ are the covariant strain components. Assuming the strain to vary linearly through the thickness, it is possible to split it into a constant membrane part and a linear bending one. The covariant strain coefficients are

$$\bar{E}_{ij} = \bar{e}_{ij} + \zeta\bar{\chi}_{ij} = \frac{1}{2}(g_{ij} - G_{ij}) + \zeta(B_{ij} - b_{ij}) \quad \text{with} \quad i,j = 1,2 \tag{24}$$

with $\zeta \in [-t/2, t/2]$, t the thickness of the shell while the metric coefficients are $g_{ij} = g_i \cdot g_j$ and $G_{ij} = \mathbf{G}_i \cdot \mathbf{G}_j$ with $i, j = 1, 2$. The curvature tensor coefficients are defined as

$$B_{ij} = -\frac{1}{2}\left(\mathbf{G}_i \cdot \mathbf{A}_{3,j} + \mathbf{G}_j \cdot \mathbf{A}_{3,i}\right) = \mathbf{G}_{i,j} \cdot \mathbf{A}_3,$$
$$b_{ij} = -\frac{1}{2}\left(g_i \cdot \mathbf{a}_{3,j} + g_j \cdot \mathbf{a}_{3,i}\right) = g_{i,j} \cdot \mathbf{a}_3.$$

A simplified third order strain measure providing the same results of the exact one can be also adopted as proposed in [4]. Adopting Voigt's notation, the covariant strain components in Eq.(24) are collected in the vector $\bar{\mathbf{E}} = [\bar{E}_{\xi\xi}, \bar{E}_{\eta\eta}, 2\bar{E}_{\xi\eta}]^T$, that, exploiting Eq.(26), becomes

$$\bar{\mathbf{E}} = \bar{\mathbf{e}} + \zeta \bar{\boldsymbol{\chi}} \tag{25}$$

with $\bar{\mathbf{e}} = [\bar{e}_{\xi\xi}, \bar{e}_{\eta\eta}, 2\bar{e}_{\xi\eta}]^T$ and $\bar{\boldsymbol{\chi}} = [\bar{\chi}_{\xi\xi}, \bar{\chi}_{\eta\eta}, 2\bar{\chi}_{\xi\eta}]^T$.

Following the isoparametric concept, geometry and displacement field are approximated, over the element, as follows

$$\mathbf{X}(\xi, \eta) = \mathbf{N}_u(\xi, \eta)\mathbf{X}_e, \quad \boldsymbol{u}(\xi, \eta) = \mathbf{N}_u(\xi, \eta)\mathbf{u}_e \tag{26}$$

where $\mathbf{X}_e$ and $\mathbf{u}_e$ collect the element control points of geometry and displacements, respectively. The matrix $\mathbf{N}_u(\xi, \eta)$ collects bivariate NURBS functions. Equation (25) in Cartesian Voigt components becomes

$$\mathbf{E} = \mathbf{e} + \zeta \boldsymbol{\chi} \tag{27}$$

and can be written in terms of generalized strains

$$\boldsymbol{\varepsilon}(\mathbf{u}_e) \equiv \begin{bmatrix} \mathbf{e} \\ \boldsymbol{\chi} \end{bmatrix} \tag{28}$$

The Jacobian of $\boldsymbol{\varepsilon}$ with respect to $\mathbf{u}_e$ furnishes the tangent strain-displacement operator in Eq.(3). The homogenized material stiffness matrix of the shell can be evaluated as

$$\mathbf{C} = \begin{bmatrix} \mathbf{C}_{ee} & \mathbf{C}_{e\chi} \\ \mathbf{C}_{e\chi}^T & \mathbf{C}_{\chi\chi} \end{bmatrix}$$

with

$$\mathbf{C}_{ee} = \sum_k t_k \mathbf{C}_k, \qquad \mathbf{C}_{e\chi} = \sum_k z_k t_k \mathbf{C}_k, \qquad \mathbf{C}_{\chi\chi} = \sum_k \left(\frac{t_k^3}{12} + t_k z_k^2\right) \mathbf{C}_k$$

where the sum is on the number of layers, t_k is the thickness of the k-th ply, z_k is the distance between the centroid of the k-th ply and the mid-plane of the laminate and $\mathbf{C}_k$ is the plane stress constitutive matrix of the generic lamina.

The same NURBS approximation used for $\boldsymbol{u}$ is employed for the velocity field $\boldsymbol{v}$, so that we can obtain the mass matrix using Eq.(6) with

$$\boldsymbol{\Xi} \equiv \rho t \begin{bmatrix} 1 & 0 & 0 \\ 0 & 1 & 0 \\ 0 & 0 & 1 \end{bmatrix} \tag{29}$$

where ρ is the mass density.

All the spatial integrals are carried out numerically by the patch-wise reduced integration to avoid membrane locking. One of the most accurate and efficient choice is the use of third order NURBS functions with C^2 inter-element continuity for which the scheme named S_0^3 proved to be the optimal numerical integration [4].

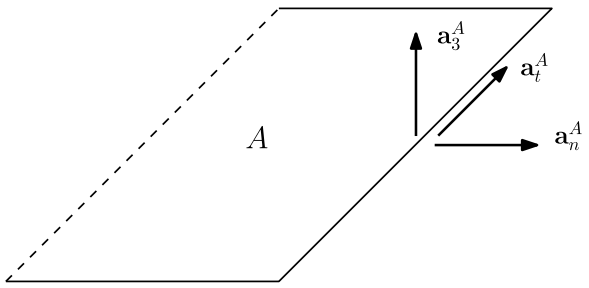

Figure 1: Illustration of vectors $\mathbf{a}_3$ and $\mathbf{a}_n$.

3.1 Penalty coupling of multiple Kirchhoff-Love shell patches

Real-world structures are typically modeled using multiple patches and, often, neither rotational continuity nor conforming discretization can be practically obtained at patch interfaces. Here, we recall a simple penalty approach for coupling adjacent patches, applicable to either smooth or non-smooth interfaces and either matching or non-matching discretizations [6, 5]. Let us assume first that there are two patches, A and B, with two edges which, in the undeformed configuration, are approximately co-located along an interface curve ℓ. For enforcing displacement continuity between the two patches, the following penalty energy [6] is added to the total energy:

$$W_d(\mathbf{u}) = \frac{1}{2}\int_\ell \alpha_d \left(\boldsymbol{u}^A - \boldsymbol{u}^B\right)^T \left(\boldsymbol{u}^A - \boldsymbol{u}^B\right) ds$$

where superscripts A and B indicate quantities evaluated on the common edge of patches A or B respectively, α_d is a penalty parameter, further discussed in the following, large enough to dictate that, if the distance between points belonging to the common edge of A and B is not the same in the deformed and undeformed configurations, a large penalty energy is introduced into the system. The coupling methodology must also maintain the angle formed by patches A and B. Analogously, for imposing rotational continuity between the two patches, using the unit vectors defined in Fig.1, the following penalty energy is further introduced:

$$\begin{aligned} W_r(\mathbf{u}) = \frac{1}{2}\int_\ell \alpha_r \Big(&\left(\mathbf{a}_3^A \cdot \mathbf{a}_3^B - \mathbf{A}_3^A \cdot \mathbf{A}_3^B\right)\left(\mathbf{a}_3^A \cdot \mathbf{a}_3^B - \mathbf{A}_3^A \cdot \mathbf{A}_3^B\right) \\ &+ \left(\mathbf{a}_n^A \cdot \mathbf{a}_3^B - \mathbf{A}_n^A \cdot \mathbf{A}_3^B\right)\left(\mathbf{a}_n^A \cdot \mathbf{a}_3^B - \mathbf{A}_n^A \cdot \mathbf{A}_3^B\right)\Big) ds \end{aligned}$$

where α_r is a large enough penalty parameter. The total coupling energy in Eq. (18) is then given by the sum

$$\Phi_c(\mathbf{u}) = W_d(\mathbf{u}) + W_r(\mathbf{u})$$

The integrals can be evaluated numerically using the interface-wise reduced integration proposed in [5], that allows to obtain accurate solutions also for non-matching meshes. A usual drawback of penalty methods is that the penalty parameters are problem dependent: they must be high enough to assure the desired coupling but not too high to generate excessive ill-conditioning. Problem dependence can be strongly reduced by taking into account geometry and material properties in the selection. For instance, in [6] it is suggested

$$\alpha_d = \alpha \frac{\max \mathbf{C}_{ee}^{ij}}{h} \qquad \alpha_r = \alpha \frac{\max \mathbf{C}_{\chi\chi}^{ij}}{h} \tag{30}$$

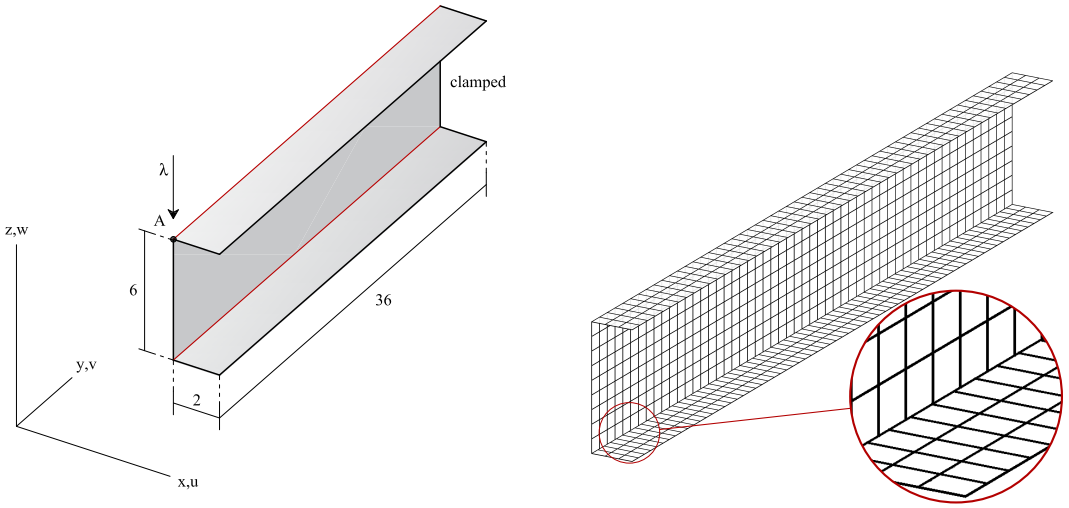

Figure 2: Thin-walled cantilever beam: geometry, boundary conditions and mesh

where α is a single penalty coefficient, $h = \frac{h^A + h^B}{2}$ with h^A and h^B the lengths of the elements in the direction most parallel to the coupling curve and $i, j = 1, 2$. The dimensionless penalty factor α becomes then the only parameter selected by the user. In this way, it was shown in [5] that values of $10^3 \leq \alpha \leq 10^6$ provide an accurate coupling in static large deformation problems without numerical problems using a mixed iterative procedure. The extension to multiple patches is trivial and requires only the addition of the corresponding coupling energies. It is worth noting that the rotational coupling law is nonlinear in $\mathbf{u}$ and is then source of non-conserving energy and instability when traditional time integration methods are used, as opposite to the new conserving proposal.

4 NUMERICAL EXAMPLES

4.1 Thin-walled cantilever beam with local buckling

A thin-walled cantilever beam with a U cross section is considered in this test. Geometry, load, boundary conditions and mesh are reported in Fig. 2. Both isotropic and composite materials are considered. The isotropic material is characterized by $E = 1.0 \times 10^7$ and $\nu = 0.3$, while for the composite material we have $E_1 = 3.06 \times 10^7$, $E_2 = E_3 = 8.70 \times 10^6$, $\nu_{12} = 0.29$, $\nu_{23} = \nu_{13} = 0.3$ and $G_{12} = G_{13} = 3.24 \times 10^6$, $G_{23} = 2.90 \times 10^6$, with the material direction 1 corresponding to the longitudinal beam axis. The thickness of the walls is 0.05, while the density per unit of volume is 10^{-2}. The approximation is based on cubic NURBS functions. In such a structure, a patch coupling strategy is necessary for the Kirchhoff-Love shell model along the red interfaces. The structure was analyzed in many previous works in statics with various shell models. In such a case, the structure is characterized by a local buckling near the clamped section after a nonlinear pre-critical path with unstable post-buckling and snap-through behavior. Here, the problem is studied form the dynamic point of view by increasing the load amplitude linearly from 0 to 150, a little higher value than the static buckling load, in 0.075 seconds. Afterwards, the load is removed linearly in 0.075 seconds and the simulation proceeds without load. The time step of the analysis is $\Delta t = 0.003125$ seconds. This is a good case to prove the energy-conserving and stability features of the proposal in a shell model with nonlinear strain measure and nonlinear coupling. The results in terms

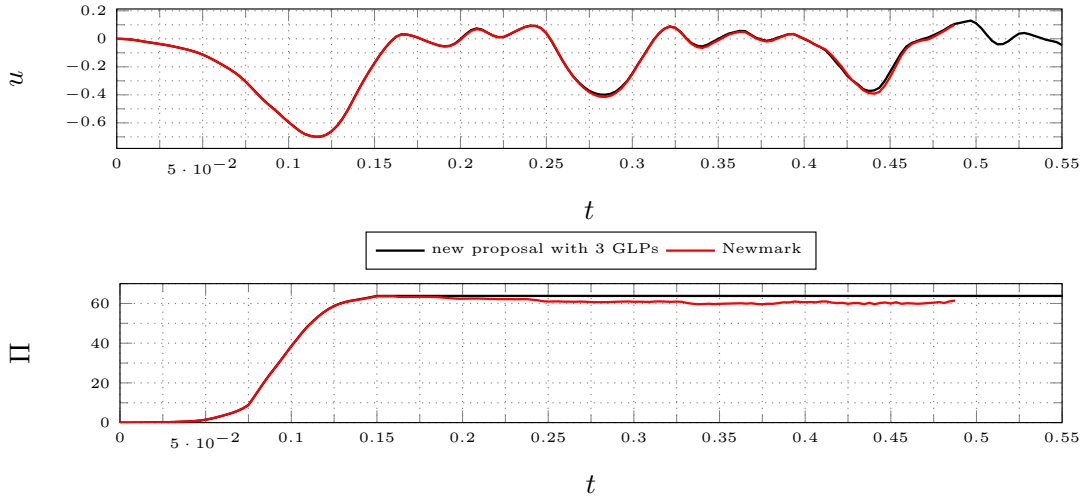

Figure 3: Thin-walled cantilever beam in isotropic material: Newmark vs new proposal

of deflection of the loaded point and of total energy of the system are reported in Fig. 3 for the isotropic case and in Fig. 4 for the composite one. We can see that the behavior of the two structures is very similar, also in terms of performance of the integration schemes. The Newmark method fails to preserve the energy after the load removal and its iterative solution fails when the energy oscillation becomes relevant. This is even more marked in the composite case with a dramatic blow-up. Instead, the proposal is perfectly stable with constant energy for a zero load and without any difficulty in the iterative solution. This is to prove the effectiveness of the proposal with generally nonlinear strain measure and coupling laws. The analysis was carried out using two values of the penalty factors, i.e. $\alpha = 10^3$ and $\alpha = 10^5$, which provide identical curves proving that the coupling law is accurately satisfied even with $\alpha = 10^3$. For the static case, accuracy and robustness of the penalty coupling in this test and others is discussed in [5]. Instead, for the dynamic case under consideration, Fig. 5 shows a comparison of the time histories provided by the non-matching Kirchhoff-Love model with penalty coupling and by a solid-shell model with exact coupling [7]. Only insignificant differences can be spotted, attributed to the different model: the solid-shell model considers solid geometry, transverse shear strains and thickness stretch.

4.2 Tumbling cylinder

The last test concerns the dynamics of a tumbling cylindrical ring in Fig. 6 made of an isotropic material with $E = 2.0 \times 10^8$, $\nu = 0.25$ and density per unit of volume equal to 0.02. Each Kirchhoff-Love patch of 8×3 cubic NURBS elements corresponds to a quarter of the ring circumference. The interface lines are orthogonal to the circumference and located at $\theta = 0$, $\theta = \pi/2$, $\theta = \pi$ and $\theta = 3\pi/2$ with θ defining the angle between the position vector of the interface mid-height point and the x axis. Four concentrated forces act at these four points as follows:

- $\mathbf{F}_1 = \begin{bmatrix} 0 & -1 & -1 \end{bmatrix}^T p(t)$ at $\theta = 0$
- $\mathbf{F}_2 = \begin{bmatrix} 1 & 1 & 1 \end{bmatrix}^T p(t)$ at $\theta = \pi/2$
- $\mathbf{F}_3 = \begin{bmatrix} 1 & 1 & 1 \end{bmatrix}^T p(t)$ at $\theta = \pi$
- $\mathbf{F}_4 = \begin{bmatrix} 0 & -1 & -1 \end{bmatrix}^T p(t)$ at $\theta = 3\pi/2$.

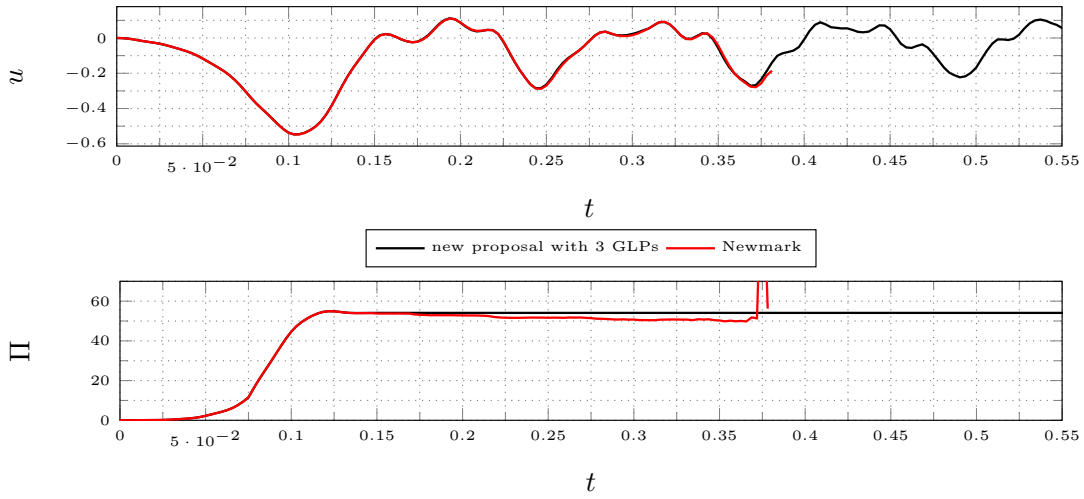

Figure 4: Thin-walled cantilever beam in composite material: Newmark vs new proposal

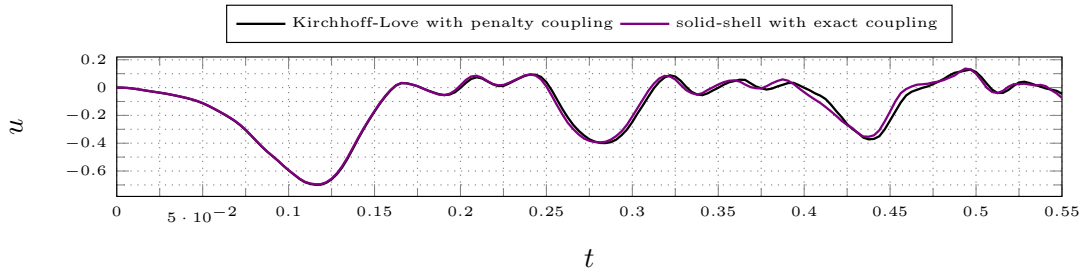

Figure 5: Thin-walled cantilever beam in isotropic material: Kirchhoff-Love model with penalty coupling vs solid-shell model with exact coupling [7]

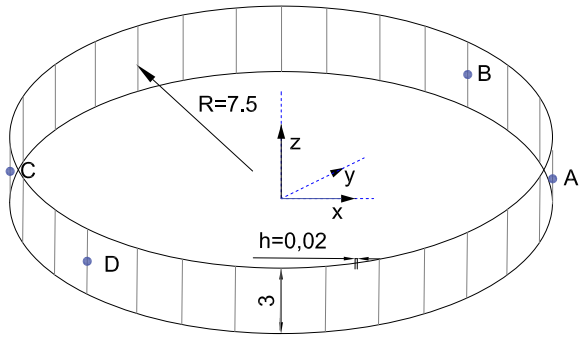

Figure 6: Tumbling cylinder: geometry

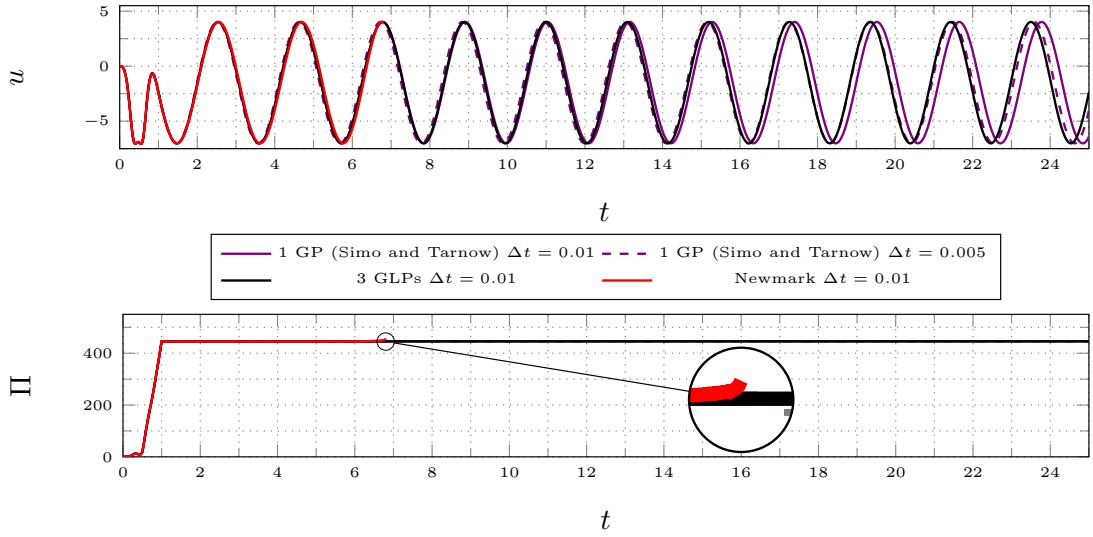

Figure 7: Tumbling cylinder: comparison of the new proposal with Newmark's trapezoidal rule and the method of Simo and Tarnow

with

$$p(t) = \begin{cases} 10t & \text{if} \quad t \leq 0.5 \\ 5 - 10(t - 0.5) & \text{if} \quad 0.5 < t \leq 1 \\ 0 & \text{if} \quad t > 1 \end{cases}$$

Figure 7 depicts the time history provided by our new scheme with 1 Gauss point over the time step (corresponding to the Simo and Tarnow method [2]) and with 3 Gauss-Lobatto points. In addition, the results of the Newmark average acceleration method are reported. We can draw the following conclusions. The Newmark method fails as soon as the energy error starts to grow significantly. The Simo and Tarnow method is only approximatively energy-conserving for the considered nonlinear model but the energy approximation is very good for this test so that the scheme is stable for the considered time steps. The new proposal with 3 Gauss-Lobatto time points conserves the energy and is also more accurate than the Simo and Tarnow one. It is important to note that the Simo and Tarnow method conserves exactly the total angular momentum for problems without external constraints such as the one under consideration. However, this conservation is not a guarantee of accuracy. Indeed, the method needs a halved time step to achieve results similar to those provided by our proposal with more time integration points.

5 CONCLUSIONS

A novel and very simple one-step time integration scheme for large deformation dynamics of elastic structures was presented. It is a generalization of the Simo and Tarnow method [2] designed to achieve unconditional stability for a quadratic strain to arbitrarily nonlinear strain measures. As in [2], the proposal uses an average internal force vector evaluated using the mean value of the stress at the end points of the time step, in order to avoid artificial straining of the intermediate configurations, and an average tangent strain-displacement operator. The difference is in the definition of this last ingredient. Instead of evaluating the average tangent strain-displacement operator as its mid-point value, we use an integral

mean over the step computed by time integration points. In this way, the method conserves energy up to the desired accuracy also for arbitrary nonlinear strain-displacement laws, resulting in unconditionally stable simulations regardless of the structural model and its spatial finite element discretization. Numerical results were illustrated regarding assemblages of Kirchhoff-Love shells with smooth and non-smooth interfaces undergoing large deformations. Unconditional stability was proven in long simulations. As opposite to the original Simo and Tarnow method, the new one does not conserves exactly the angular momentum. Interestingly, this last feature seems to be marginal in practical computations. Energy conservation assures stability. Conserving the angular momentum neither implies stability nor is synonym of higher accuracy. This is highlighted in the last test, where the momentum-conserving scheme needs a halved time step to get the same accuracy in displacements compared to our energy-conserving scheme. More details are available in [8], together with many other numerical tests concerning also Reissner beams.

REFERENCES

[1] Betsch, P. and Steinmann, P. Conservation properties of a time FE method. Part I: time-stepping schemes for N-body problems. *Int. J. Numer. Meth. Engng.* (2000) **49**: 599–638.

[2] Simo, J.C. and Tarnow, N. The discrete energy-momentum method. Conserving algorithms for nonlinear elastodynamics. *Z. angew. Math. Phys.* (1992) **43**: 757–792.

[3] Sansour, C. and Wriggers, P. and Sansour, J. Nonlinear Dynamics of Shells: Theory, Finite Element Formulation, and Integration Schemes. *Nonlinear Dynamics* (1997) **17**: 279–305.

[4] Leonetti, L. and Magisano, D. and Madeo, A. and Garcea, G. and Kiendl, J and Reali, A. A simplified Kirchhoff–Love large deformation model for elastic shells and its effective isogeometric formulation. *Computer Methods in Applied Mechanics and Engineering* (2019) **354**: 369–396.

[5] Leonetti, L. and Liguori, F. S. and Magisano, D. and Kiendl, J and Reali, A. and Garcea, G. A robust penalty coupling of non-matching isogeometric Kirchhoff–Love shell patches in large deformations. *Computer Methods in Applied Mechanics and Engineering* (2020) **371**: 113289.

[6] Austin J. Herrema, Emily L. Johnson, Davide Proserpio, Michael C.H. Wu, Josef Kiendl, Ming-Chen Hsu, Penalty coupling of non-matching isogeometric Kirchhoff–Love shell patches with application to composite wind turbine blades. *Computer Methods in Applied Mechanics and Engineering* (2019) **346**: 810–840.

[7] Leonetti, L. and Liguori, F. S. and Magisano, D. and Garcea, G. An efficient isogeometric solid-shell formulation for geometrically nonlinear analysis of elastic shells. *Computer Methods in Applied Mechanics and Engineering* (2018) **331**: 159–183.

[8] Magisano, D. and Leonetti, L. and Garcea, G. Unconditional stability in large deformation dynamic analysis of elastic structures with arbitrary nonlinear strain measure and multi-body coupling. *Computer Methods in Applied Mechanics and Engineering* (2022) **393**: 114776.